

ChemComm

Accepted Manuscript



This is an *Accepted Manuscript*, which has been through the Royal Society of Chemistry peer review process and has been accepted for publication.

Accepted Manuscripts are published online shortly after acceptance, before technical editing, formatting and proof reading. Using this free service, authors can make their results available to the community, in citable form, before we publish the edited article. We will replace this *Accepted Manuscript* with the edited and formatted *Advance Article* as soon as it is available.

You can find more information about *Accepted Manuscripts* in the [Information for Authors](#).

Please note that technical editing may introduce minor changes to the text and/or graphics, which may alter content. The journal's standard [Terms & Conditions](#) and the [Ethical guidelines](#) still apply. In no event shall the Royal Society of Chemistry be held responsible for any errors or omissions in this *Accepted Manuscript* or any consequences arising from the use of any information it contains.

Cite this: DOI: 10.1039/c0xx00000x

www.rsc.org/xxxxxx

Communication**Polymeric Micelle Assembly for Direct Synthesis of Functionalized Mesoporous Silica with Fully Accessible Pt Nanoparticles toward Improved CO Oxidation Reaction**Bishnu Prasad Bastakoti¹, Yunqi Li^{1,2}, Nobuyoshi Miyamoto³, Hideki Abe⁴, Jinhua Ye⁴, Pavuluri Srinivasu^{1,5}, and Yusuke Yamauchi^{1,2*}

Received (in XXX, XXX) Xth XXXXXXXXXX 20XX, Accepted Xth XXXXXXXXXX 20XX

DOI: 10.1039/b000000x

Pt-decorated mesoporous silica is directly prepared using polymeric micelles assembly approach using an asymmetric triblock copolymer, poly(styrene-*b*-2-vinylpyridine-*b*-ethylene oxide) as structure directing agent. Strongly immobilized, fully accessible, and uniformly dispersed Pt nanoparticles on mesoporous silica wall exhibit superior catalytic activity toward CO oxidation.

Noble metal nanoparticles supported on inorganic substances (*i.e.*, carbon, metal oxides) exhibit high catalytic activity for a wide range of chemical reactions.¹ Colloidal chemistry has enabled the synthesis of catalytically active metal nanoparticles with tunable shapes, sizes, and compositions. The colloidal nanoparticles are usually prepared in the presence of organic capping agent that prevent the aggregation of nanoparticles in the solution.² Several industrially important reactions, such as CO oxidation,³ isomerization,⁴ cross-coupling⁵, are carried out at higher temperature. At high temperature, the organic capping agents decompose and metal nanoparticles can deform and aggregate each other. Their performance at high temperature is different from those of pristine metal nanoparticles. Recently, many efforts have been made to prepare the very stable metal catalysts that can be used at high temperature. Deposition of metal nanoparticles on/into porous materials as supports helps to prevent the aggregation of neighbouring nanoparticles even at high temperature.⁶ Chemical vapor deposition,⁷ photo irradiation,⁸ sol-gel,⁹ and sputtering¹⁰ have been utilized for the effective dispersion of metal nanoparticles over the supports. Addition of metal sources into porous substrates and their subsequent reduction are also very common method to introduce the metal nanoparticles into/on the porous matrix.¹¹

Post-treatment is well-known approach for deposition of metal nanoparticles on inorganic matrix. Pt-supported catalysts are synthesized by typical impregnation and subsequent hydrogen reduction method. However, Pt nanoparticles located inside the mesopores are often non uniform and their particle size distributions are broad.^{12,13} Several mesoporous metal oxides (*i.e.*, silica, alumina) have been loaded with size-controlled Pt nanoparticles to investigate the effects of oxide-metal interface on catalytic CO oxidation reaction.¹⁴ Growth of mesoporous silica shell on metal nanoparticles has been also reported.¹⁵ Thermally stable mesoporous silica shell providing direct access to the Pt core makes an efficient catalyst for hydrogenation and CO oxidation. In spite of the above progress, complicated synthetic systems are still required. Size-control of metal nanoparticles and selection of reducing agent and/or capping agent makes the method more complicated. Also, serious pore blocking by metal

nanoparticles has been sometimes observed, which drastically reduces the performance of materials.

Here, we synthesized Pt-decorated mesoporous silica in which the Pt nanoparticles are strongly anchored on the silica wall, by assembly of spherical polymeric micelles consisting of poly(styrene-*b*-2-vinylpyridine-*b*-ethylene oxide) (PS-*b*-PVP-*b*-PEO) block copolymer with three chemically distinct units (Fig. 1). Our polymeric micelle assembly is totally different from traditional evaporation-induced self-assembly (EISA).¹⁶ Strong hydrophobic interaction of platinum(II) 2,4-pentanedionate with the PS core and acid-catalyzed polymerization of silica precursor on the PVP shell enable us to directly synthesize Pt-decorated mesoporous silica. The hydrophobic PS block is kinetically frozen in the precursor solution, enabling the spherical micelles to remain in a stable form. The frozen PS core serves as template and the thermally stable block copolymer prevents collapse of ordered mesostructure during calcination process. The platinum source is *in-situ* converted to the Pt nanoparticles on silica walls without use of any reducing agents. Our Pt-decorated mesoporous silica exhibits the excellent performance for the oxidation of CO.

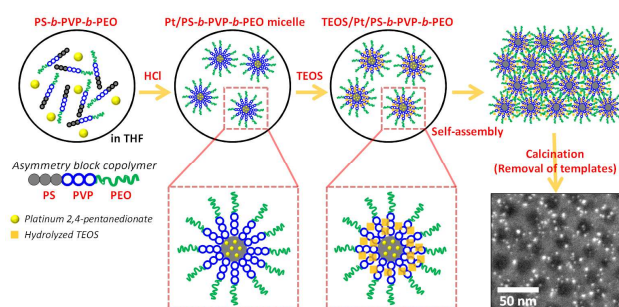


Fig. 1 Illustration of synthetic process of Pt-decorated mesoporous silica by 'polymeric micelle assembly'.

In this experimental, PS₍₁₃₀₀₀₎-*b*-PVP₍₉₀₀₀₎-*b*-PEO₍₁₆₅₀₀₎ block copolymer (20 mg) and platinum(II) 2,4-pentanedionate (15 mg) were dissolved into THF (4.0 mL) ultrasonically (The numbers inside parentheses indicate the molecular weight of each block). No micelles or nanoaggregates were detected by dynamic light scattering (DLS) measurement. After addition of HCl solution (80 μ L), the micellization occurred as a result of insolubilization of the PS core in HCl solution. Slow addition of HCl solution is important to form uniform-sized polymeric micelles. Hydrophobic Pt source was encapsulated in the PS core due to hydrophobic interaction. It has been known that hydrophobic organic dyes and metal sources can easily

incorporate into hydrophobic domain of micelles.¹⁷ The Tyndall effect on the solution is one of the evidence for the formation of micelles (Fig. S1-a). Furthermore, we directly visualized the presence of polymeric micelles by confocal laser scanning microscope (Fig. S1-b). Uniformly-sized polymeric micelles showed Brownian motion in the solution, which is the direct evidence of the formation of very stable and highly uniform micelles. From dynamic light scattering experiment (DLS), it was found that the average hydrodynamic diameter was 80 ± 5 nm with polydispersity index 0.09. The zeta-potential measurements revealed that the micelles possessed positive surface charge of 35 mV. Tetraethoxysilane (100 μ L) was added into the micelles solution and stirred for 3 hours at room temperature; the hydrolyzed silica precursors were interacted on the PVP shell. Thus, the PVP shell serves as reaction site for sol-gel reaction according to Nakashima's report.¹⁸ The zeta-potential was again measured and it was significantly decreased to 5 mV, indicating that the polymerization of silica sources on PVP shell masks its positive charge. The hydrodynamic diameter of the obtained composite micelles was about 60 nm. The resulting solution containing of polymeric micelles was dried in room temperature by keeping on open Petri dish. After complete solvent evaporation, the sample was calcined at 600 °C in N₂ environment. From the thermogravimetric analysis (TGA) curves of the polymer and polymer composites in N₂ flow (Fig. S2), a sharp weight loss was confirmed at around 500 °C, indicating complete combustion of the polymer and derivatives (carbon).

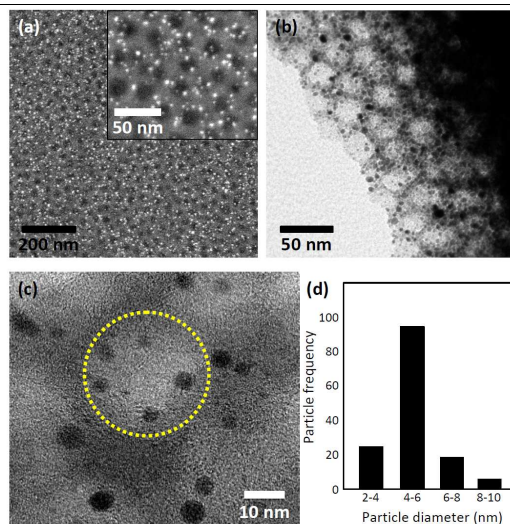


Fig. 2 (a) SEM and (b and c) low- and high-magnified TEM images of Pt-decorated mesoporous silica (One mesopore is indicated by a yellow-colored circle.), and (d) particle size distribution of Pt nanoparticles deposited inside the mesopores.

The calcination process not only removes the polymer template but also deposits Pt nanoparticles. In general, selection of reducing agent is another troublesome for the synthesis of uniformly sized Pt nanoparticles, because the nanoparticle sizes strongly depend on the kinetics of reduction.¹⁹ In the present study, Pt source is thermally converted to metallic Pt nanoparticles without using any reducing agent. The *in-situ* formed carbon from polymer during calcination in inert medium reduces the Pt precursors to Pt nanoparticles and deposits on mesoporous silica support.^{17b, 17c}

After removing the micelle template, orderly arranged mesoporous silica with uniformly distributed Pt nanoparticles was obtained. The average size of mesopores and the wall

thicknesses are *ca.* 25 nm and *ca.* 15 nm, respectively as shown in Fig. 2a-c. The pore size corresponds to the PS core of polymeric micelles. Therefore, changing the molecular weights of PS blocks can easily control the mesopore sizes of the products.²⁰ The detailed location of Pt nanoparticles on the mesoporous silica was clearly observed by TEM (Fig. 2b and 2c). Small-sized Pt nanoparticles were distributed through out the mesoporous wall. The particle size distribution for Pt nanoparticles is shown in Fig. 2d. The particles size distribution was obtained by accounting 150 Pt nanoparticles in different TEM images. Most of the particles were about 4-6 nm in diameter.

The porosity of Pt-decorated mesoporous silica was investigated by N₂ adsorption-desorption isotherm. The isotherm exhibited type IV with hysteresis loop, which is typical of mesoporous materials. Large uptake was clearly observed in high relative pressure range from 0.8 to 0.9, because the mesopore size is relatively large. The BET surface area was calculated to be 64 m²·g⁻¹ with average pore size 30 nm (Fig. S3). This surface area is lower compared to other mesoporous silica materials without Pt nanoparticles, but this situation is acceptable. The addition of Pt content largely decreased the mass-normalized surface area because Pt is a heavy element. From wide-angle XRD pattern (Fig. S4a), several diffraction peaks were observed. These peaks can be assigned to (111), (200), (220), (311), and (222) peaks of *fcc* Pt crystal. The presence of metallic Pt nanoparticles in mesoporous silica was also confirmed by X-ray photoelectron spectroscopy. The main peaks with the binding energy of Pt 4f_{5/2} at 74.58 eV and Pt 4f_{7/2} at 71.08 eV are typical for the zero valent Pt (Fig. S4b). The additional peaks at 76.18 eV and 72.08 eV were necessary to fit the experimental data. These peaks could be assigned to Pt(II) related to PtO. Oxygen chemisorption may occur at step and kink sites present on the surface of the Pt nanoparticles.²¹

The most inevitable problem associated with catalysts in the industrial use is thermal agglomeration of the catalytic centres at high temperatures, which greatly retards the catalytic performance. Our Pt-decorated mesoporous silica prepared in this study is free from such substantial thermal agglomeration, because the nanoparticles are strongly anchored on the silica wall. This strongly immobilization of nanoparticles on silica wall inhibits serious nanoparticle sintering and loss of catalytic activity even after prolonged heating at high temperatures (Fig. S5). As preliminary application of Pt-decorated mesoporous silica as catalyst, we investigated its catalytic activity toward the oxidation of CO by O₂. Here the CO oxidation reaction was performed over the catalyst in a circulating-gas reactor equipped with a gas chromatograph. The catalyst was vacuum-dried in the reactor at 150 °C prior to the reaction. Then, mixture of CO (6.67 kPa) and O₂ (3.33 kPa) was circulated through the catalyst. The formation of CO₂ was monitored by gas chromatography. Our Pt-incorporated mesoporous silica efficiently catalyzed the CO oxidation at 150 °C and interestingly achieved full conversion of CO to CO₂ within a couple of minutes (Fig. 3). For comparison, we tested standard Pt/SiO₂ catalyst where Pt nanoparticles are deposited on silica spheres.²² Obviously, time course of CO conversion over Pt-incorporated mesoporous silica exhibited higher CO conversion at any duration. Therefore, the mesoporous silica walls not only stabilize the Pt nanoparticles but also provide easy access to the Pt nanoparticle surface, thereby serving as an efficient catalyst.

To further demonstrate wide applicability of 'polymeric micelle assembly', we changed inorganic substrate from silica to alumina (Al₂O₃). Porous alumina also represents one of the most prominent inorganic supports for noble metals that are widely applied as catalyst in several reactions.²³ For this preparation,

aluminium butoxide was used instead of TEOS to synthesize Pt-decorated mesoporous alumina. Fig. S6 shows the strong anchoring of Pt nanoparticles on the alumina wall. The particle size distribution of deposited Pt nanoparticles was similar as that of Pt-decorated mesoporous silica. We believe that our approach will be easily extendable to synthesize other compositions.

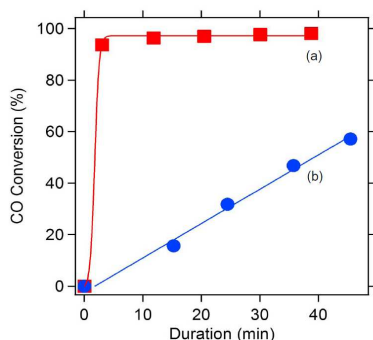


Fig. 3 CO oxidation by using (a) Pt-decorated mesoporous silica and (b) standard Pt/SiO₂ catalyst. The activity of CO conversion is normalized with the mass of Pt nanoparticles in the samples.

In conclusion, Pt-decorated mesoporous silica is directly prepared using polymeric micelle assembly approach using an asymmetric triblock copolymer, poly(styrene-*b*-2-vinylpyridine-*b*-ethylene oxide) as structure directing agent. Introduction of hydrophobic Pt source into the PS core and acid-catalyzed polymerization reaction of silica precursor on PVP shell enable to directly synthesize Pt-decorated mesoporous silica. Our approach based on 'polymeric micelle assembly' is simple and advantage for deposition of fully accessible and uniformly dispersed metal nanoparticles on/into the mesopores. Pt-decorated mesoporous silica obtained in this study showed superior catalytic activity for the oxidation of CO than standard Pt/SiO₂ catalyst. The simplicity, flexibility, and reproducibility of our synthetic method allow easy fabrication of various mesoporous materials with different metal nanoparticles and different framework compositions in future.

Acknowledgments

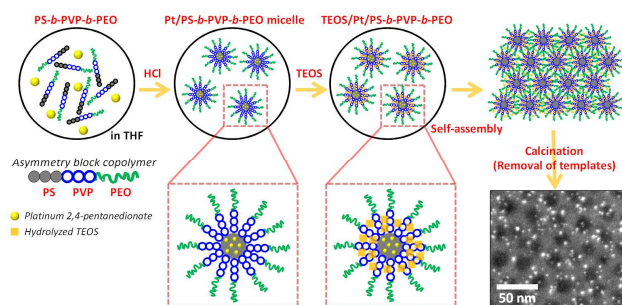
This research is supported by the Japan Society for the Promotion of Science.

- World Premier International (WPI) Research Center for Materials Nanoarchitectonics, National Institute for Materials Science (NIMS), 1-1 Namiki, Tsukuba, Ibaraki 305-0044, Japan.
- Faculty of Science and Engineering, Waseda University, 3-4-1 Okubo, Shinjuku, Tokyo 169-8555, Japan.
- Department of Life, Environment, and Materials Science, Faculty of Engineering, Fukuoka Institute of Technology (FIT), 3-30-1 Wajiro-Higashi, Higashi, Fukuoka 811-0295, Japan.
- Environmental Remediation Materials Unit, National Institute for Materials Science (NIMS), 1-1 Namiki, Tsukuba, Ibaraki 305-0044, Japan.
- Inorganic and Physical Chemistry Division, Indian Institute of Chemical Technology (IICT), Tarnaka, Hyderabad-500 007, India.
E-mail: Yamauchi.Yusuke@nims.go.jp

References

- (a) A. Chen and P. H. Hindle, *Chem. Rev.*, 2010, **110**, 3767-3804. (b) A. Fukuoka, J. Kimura, T. Oshio, Y. Sakamoto and M. Ichikawa, *J. Am. Chem. Soc.*, 2007, **129**, 10120-10125. (c) C. Zhang, S. Li, T. Wang, G. Wu, X. Ma and J. Gong, *Chem. Commun.*, 2013, **49**, 10647-10649. (d) L. V. Mattos, G. Jacobs, B. H. Davis and F. B. Noronha, *Chem. Rev.*, 2012, **112**, 4094-4123. (e) D. Varade, H. Abe, Y. Yamauchi and K. Haraguchi, *ACS Appl. Mater. Interface.*, 2013, **5**, 11613-11617.
- Z. Niu and Y. Li, *Chem. Mater.*, 2014, **26**, 72-83.
- M. Comotti, W.-C. Li, B. Spliethoff and F. Schüth, *J. Am. Chem. Soc.*, 2006, **128**, 917-924.
- X. Han and D. W. Armstrong, *Org. Lett.*, 2005, **7**, 4205-4208.
- B. Karimi and F. K. Esfahani, *Chem. Commun.*, 2011, **47**, 10452-10454.
- G. Gupta, M. N. Patel, D. Ferrer, A. T. Heitsch, B. A. Korgel, M. J. Yacaman and K. P. Johnston, *Chem. Mater.*, 2008, **20**, 5005-5015.
- M. Seipenbusch and A. Binder, *J. Phys. Chem. C*, 2009, **113**, 20606-20610.
- B. P. Bastakoti, K. C.-W. Wu and Y. Yamauchi, *J. Nanosci. Nanotechnol.*, 2013, **13**, 2735-2739.
- B. P. Bastakoti, S. Guragain, S. Yusa and K. Nakashima, *RSC Advances*, 2012, **2**, 5938-5940.
- L. Armelao, D. Barreca and G. Bottaro, A. Gasparotto and E. Tondello, M. Ferroni and S. Polizzi, *Chem. Mater.*, 2004, **16**, 3331-3338.
- H. Wang, H.Y. Jeong, M. Imura, L. Wang, L. Radhakrishnan, N. Fujita, T. Castle, O.Terasaki and Y. Yamauchi, *J. Am. Chem. Soc.*, 2011, **133**, 14526-14529.
- A. Fukuoka, J. Kimura, T. Oshio, Y. Sakamoto and M. Ichikawa, *J. Am. Chem. Soc.*, 2007, **129**, 10120-10125.
- L. Nie, A. Meng, J. Yu and M. Jaroniec, *Sci. Rep.*, 2013, **3**, 3215-3220.
- K. An, S. Alayoglu, N. Musselwhite, S. Plamthottam, G. Melaet, A. E. Lindeman and G. A. Somorjai, *J. Am. Chem. Soc.*, 2013, **135**, 16689-16696.
- S. H. Joo, J. Y. Park, C.-K. Tsung, Y. Yamada, P. Yang and G. A. Somorjai, *Nat. Mater.*, 2009, **8**, 126-131.
- Firstly, a homogeneous solution is prepared by mixing soluble silica and surfactant with ethanol/water solvent. During preferential evaporation of ethanol, the surfactant concentration is gradually increased. This progressively increasing surfactant concentration drives self-assembly of silica/surfactant micelles and their further organization into well-defined liquid crystalline mesophases-which can serve as templates.
- (a) B. P. Bastakoti, K. C.-W. Wu, M. Inoue, S. Yusa, K. Nakashima and Y. Yamauchi, *Chem. Euro. J.*, 2013, **19**, 4812-4817 (b) B. P. Bastakoti, N. L. Torad and Y. Yamauchi, *ACS Appl. Mater. Inter.*, 2014, **6**, 854-860 (c) M. C. Orilall, F. Matsumoto, Q. Zhou, H. Sai, H. D. Abruna, F. J. DiSalvo and U. Wiesner, *J. Am. Chem. Soc.*, 2009, **131**, 9389-9395. (d) B. P. Bastakoti, Y. Hsu, S. Liao, K. C.-W. Wu, M. Inoue, S. Yusa, K. Nakashima and Y. Yamauchi, *Chem. Asian J.*, 2013, **8**, 1301-1305.
- A. Khanal, Y. Inoue, M. Yada and K. Nakashima, *J. Am. Chem. Soc.*, 2007, **129**, 1534-1535.
- N. G. Bastus, J. Comenge and V. Puentes, *Langmuir*, 2011, **27**, 11098-11105.
- B. P. Bastakoti, S. Ishihara, S. Y. Leo, K. Ariga, K. C.-W. Wu and Y. Yamauchi, *Langmuir*, 2014, **30**, 651-659.
- (a) C. R. Parkinson, M. Walker and C. F. McConville, *Surf. Sci.*, 2003, **545**, 19-33. (b) C. Dablemont, P. Lang, C. Mangeney, J.-Y. Piquemal, V. Petkov, F. Herbst and G. Viau, *Langmuir*, 2008, **24**, 5832-5841. (c) H. Kong, M. Zhou, G.-D. Lin and H.-B. Zhang, *Catal Lett*, 2010, **135**, 83-90.
- An aliquot of 292.6 ml of aqueous H₂PtCl₆ (Tanaka Kikinzoku Co. Ltd.) solution (0.3 wt. %) was added slowly into 300 ml of 22.5 mmol aqueous polyvinylpyrrolidone (Nakaraites Co. Ltd) solution. After vigorous stirring, 150 ml of ethanol was added to the solution and then refluxed for 6 h at 100° C. The yellowish precursor solution turned black during reflux. The solution was then condensed by distillation under reduced pressure to leave a black colored solution. The concentration of Pt in the solution was determined to be 0.62 wt. % by Inductively-coupled plasma mass spectroscopy analysis. An aliquot of 1.0 wt. % of Pt nanoparticles relative to the amount of SiO₂ was then added to a water suspension of SiO₂ (20 g of SiO₂ in 200 ml of ion-exchange water). After removal of the supernatant, the residue was dried for 2 h at 120 °C. The final product was crushed and annealed at 450 °C in air for 2 h to yield the desired catalyst.
- (a) M. Arenz, K. J. J. Mayrhofer, V. Stamenkovic, B. B. Blizanac, T. Tomoyuki, P. N. Ross and N. M. Markovic, *J. Am. Chem. Soc.*, 2005, **127**, 6819-29. (b) B. Roldan Cuenya, J. R. Croy, S. Mostafa, F. Behafarid, L. Li, Z. Zhang, J. C. Yang, Q. Wang and A. I. Frenkel, *J. Am. Chem. Soc.*, 2010, **132**, 8747-56. (c) E. Schmidt, A. Vargas, T. Mallat and A. Baiker, *J. Am. Chem. Soc.*, 2009, **131**, 12358-67.

Table of contents



5 Bishnu Prasad Bastakoti, Yunqi Li, Nobuyoshi Miyamoto, Hideki Abe, Jinhua Ye, Pavuluri Srinivasu^{1,5}, and Yusuke Yamauchi*